Volume 50(6): 839–850, 2002
The Journal of Histochemistry & Cytochemistry
http://www.jhc.org

ARTICLE

Effects of Infantile/Prepubertal Chronic Estrogen Treatment and Chemical Sympathectomy with Guanethidine on Developing Cholinergic Nerves of the Rat Uterus

Analía Richeri, Lorena Viettro, Rebeca Chávez–Genaro, Geoffrey Burnstock, Timothy Cowen, and M. Mónica Brauer

Laboratorio de Biología Celular, Instituto de Investigaciones Biológicas Clemente Estable, Montevideo, Uruguay (AR,LV,RCG,MMB); Departamento de Histología, Facultad de Medicina, Montevideo, Uruguay (RCG); Autonomic Neuroscience Institute, Royal Free and University College Medical School, London, United Kingdom (GB); and Department of Anatomy and Developmental Biology, Royal Free and University College Medical School, London, United Kingdom (TC)

SUMMARY The innervation of the uterus is remarkable in that it exhibits physiological changes in response to altered levels in the circulating levels of sex hormones. Previous studies by our group showed that chronic administration of estrogen to rats during the infantile/prepubertal period provoked, at 28 days of age, an almost complete loss of norepinephrine-labeled sympathetic nerves, similar to that observed in late pregnancy. It is not known, however, whether early exposure to estrogen affects uterine cholinergic nerves. Similarly, it is not known to what extent development and estrogen-induced responses in the uterine cholinergic innervation are affected by the absence of sympathetic nerves. To address this question, in this study we analyzed the effects of infantile/prepubertal chronic estrogen treatment, chronic chemical sympathectomy with guanethidine, and combined sympathectomy and chronic estrogen treatment on developing cholinergic nerves of the rat uterus. Cholinergic nerves were visualized using a combination of acetylcholinesterase histochemistry and the immunohistochemical demonstration of the vesicular acetylcholine transporter (VAChT). After chronic estrogen treatment, a well-developed plexus of cholinergic nerves was observed in the uterus. Quantitative studies showed that chronic exposure to estrogen induced contrasting responses in uterine cholinergic nerves, increasing the density of large and medium-sized nerve bundles and reducing the intercept density of fine fibers providing myometrial and perivascular innervation. Estrogen-induced changes in the uterine cholinergic innervation did not appear to result from the absence/impairment of sympathetic nerves, because sympathectomy did not mimic the effects produced by estrogen. Estrogen-induced responses in parasympathetic nerves are discussed, considering the direct effects of estrogen on neurons and on changes in neuron–target interactions. **(J Histochem Cytochem 50:839–850, 2002)**

KEY WORDS
uterus
estrogen
sympathectomy
plasticity
cholinergic nerves
acetylcholinesterase
vesicular acetylcholine transporter

Several studies have shown that the innervation of the uterus is dynamic and demonstrates considerable remodeling during puberty (Brauer et al. 1992), estrous cycle (Adham and Schenk 1969; Marshall 1981; Traurig and Papka 1992; Melo and Machado 1993; Zoubina et al. 1998), and pregnancy (Stjernquist et al. 1985; Owman and Stjernquist 1988; Haase et al. 1997), and after manipulations such as ovariectomy and/or exogenous sex hormone administration (McKercher et al. 1973; Juorio et al. 1989; Zoubina et al. 2001).

Previous studies by our group showed that hormone-induced plasticity of uterine nerves is not restricted to the mature state. Chronic administration of estrogen to rats during the infantile/prepubertal period provokes, at 28 days of age, an almost complete

Correspondence to: Dr. M.M. Brauer, Laboratorio de Biología Celular, Instituto de Investigaciones Biológicas Clemente Estable, Avenida Italia 3318, Montevideo 11600, Uruguay. E-mail: brauer@iibce.edu.uy

Received for publication September 12, 2001; accepted January 9, 2002 (1A5639).

0022-1554/02/$3.30

loss of norepinephrine histofluorescent-labeled sympathetic nerves and reduces by 80% the total content of norepinephrine (NE) in the uterine horn (Brauer et al. 1995,1999). It is not known, however, whether chronic exposure to estrogen affects the development of uterine cholinergic nerves.

Considering that sympathetic nerves appear to exert either positive effects (Sharp and Smith 1992; Smith and Marzban 1998) or negative effects (Aberdeen et al. 1992) on parasympathetic nerve outgrowth, and taking into account that trophic interactions may exist between parasympathetic and sympathetic nerves (Hasan and Smith 2000), we analyzed whether development and estrogen-induced responses in uterine cholinergic innervation are affected by sympathectomy.

In this study we analyzed the effects of infantile/prepubertal chronic estrogen treatment, chronic chemical sympathectomy with guanethidine, and combined chronic sympathectomy and chronic estrogen treatment on the development of the cholinergic innervation of the rat uterus. Cholinergic nerves were demonstrated using a combination of acetylcholinesterase (AChE) histochemistry and the immunohistochemical demonstration of the specific cholinergic marker vesicular acetylcholine transporter (VAChT) (Arvidsson et al. 1997; Schäfer et al. 1998). Because AChE histochemistry has been considered to be a nonspecific marker for cholinergic nerves (Papka et al. 1981,1999; Garfield 1986) a comparative assessment of the pattern of labeling given by both techniques was carried out on selected uterine tissue sections.

Materials and Methods

Animals and Treatments

Forty-two female Wistar-derived albino rats from the breeding colony held at the Instituto de Investigaciones Biológicas Clemente Estable (Montevideo, Uruguay) were used in this study. Animals were sexed at birth, weaned at 3 weeks, and maintained under controlled conditions of temperature and illumination, with water and food ad libitum.

Females were injected daily (Monday to Friday) with 50 mg/kg of guanethidine monosulfate (Sigma; St Louis, MO) from 8 days after birth and for 3 weeks (Brauer et al. 1994). Guanethidine was dissolved to appropriate doses with 0.1 M PBS and was administrated SC. Control animals from matched litters were injected with the vehicle.

Chronic estrogen treatment was performed with β-estradiol 17-cypionate (Laboratorios Köning; Buenos Aires, Argentina), diluted to appropriate doses with peanut oil (Sigma) to a final volume of 0.1 ml per dose. Intact and sympathectomized animals were injected SC with four doses of 10 μg estrogen on Days 10, 15, 20, and 25 of postnatal development. Control animals from matched litters were injected with 0.1 ml of peanut oil per dose. All animal groups were sacrificed at 28 days of age (Brauer et al. 1995,1999).

Histochemistry and Immunohistochemistry

Animals were terminally anesthetized with sodium pentobarbital (50 mg/kg IP; Sigma) and perfused via the left ventricle with 25 ml of heparinized saline solution (NaCl 0.9% + 50 IU/ml of Liquemine; Roche, Montevideo, Uruguay). Surgical procedures were conducted in accordance with the international guidelines for animal care approved in 2000 by the Instituto de Investigaciones Biológicas Clemente Estable, Montevideo, Uruguay.

For preparation of whole mounts, the uterine horns were removed, cut in 1-cm-long segments, and opened longitudinally along their parametrial border. The endometrium was carefully removed and the width of the isolated myometrium was measured before and after stretching. Stretched whole mounts were fixed in buffered 4% paraformaldehyde (PFA) (Sigma) for 25 min at 4C and then processed for histochemical demonstration of AChE. In view of the irregular penetration of VAChT antiserum and the high background observed in whole-mount preparations of estrogen-treated animals, immunostained whole mounts were not employed for quantitative studies.

For cryostat sections, animals were anesthetized and perfused transcardiacally with 25 ml of heparinized saline solution followed by 25 ml of PFA. The uterine horns were removed and fixed by immersion in 4% PFA for 1.5 additional hr at 4C. Tissues were washed in PBS, stored in 20% sucrose in PBS overnight at 4C, and embedded in tissue freezing medium (Shandon; Pittsburgh, PA). Cryostat sections (12 μm thick) were mounted on gelatin-subbed glass slides and processed for histochemical demonstration of AChE or immunohistochemical localization of VAChT. The quality of sympathectomy was assessed on adjacent sections immunostained for tyrosine hydroxylase (TH) (Brauer et al. 1999).

For demonstration of AChE activity, whole-mount preparations and cryostat tissue sections were incubated for 2 hr at 37C in a medium containing acetylthiocholine iodide (Sigma) as substrate (Karnovsky and Roots 1964) and 10^{-4} M tetraisopropyl phosphoramide (iso-OMPA; Sigma) as nonspecific cholinesterases inhibitor. Preparations were examined with a Nikon E800 microscope and micrographs were taken with Ilford PAN F, 50 ASA film.

For immunohistochemistry, sections were incubated overnight in a humid chamber at room temperature (RT) with goat anti-rabbit VAChT (1:1000 final dilution; Chemicon, Temecula, CA) or rabbit anti-tyrosine hydroxilase (1:200; Affinity Research Products, Exeter, UK). At the end of the incubation period, sections were washed in PBS, incubated with donkey anti-goat (for VAChT) or goat anti-rabbit (for TH) conjugated with Alexa-Fluor 488 (final dilution 1:400; Molecular Probes, Eugene, OR) for 1.5 hr at RT, washed in PBS, and mounted in antifade mountant (Citifluor; London, UK). Sections were examined with a Nikon E800 microscope equipped with epifluorescence and fitted with the appropriate filters. Micrographs were taken with Ilford HP5, 400 ASA film.

For double-labeling experiments, sections were stained first for AChE, mounted in Citifluor, and photographed under the microscope. After removing the coverslips, sections were washed in PBS and processed for immunohistochemistry as described above. Digital images were captured using a

CoolSNAP-Pro Monochrome Digital Kit (Media Cybernetics; Silver Spring, MD), processed with the Image-Pro Plus software (Media Cybernetics), and printed on Hewlett Packard HP Premium Inkjet glossy paper using a Hewlett Packard Deskjet 840C printer.

Nerve Diameter and Nerve Density Measurements

Nerve diameter and nerve density measurements were carried out on whole-mount stretch preparations stained for AChE. Whole-mount preparations rather than cryostat tissue sections were selected for quantitation because they allowed more accurate discrimination between perivascular and myometrial nerve fibers. Because of the uneven regional distribution of AChE-positive nerves in the rat uterus (see Results), measurement studies were restricted to the caudal region of the uterine horn. Two to four whole-mount preparations per animal were used for quantitation. For all parameters and areas analyzed, data recorded from each animal were averaged and the resulting number was used to calculate mean values.

The diameter of nerve bundles and of myometrial and perivascular nerve fibers was assessed directly under the microscope using an ocular scale and a ×40 objective lens. An average of 100 nerves per animal were measured.

The intercept density of nerve bundles and myometrial nerve fibers was estimated directly under the microscope using a 1-mm-long ocular scale set perpendicular to the uterine long axis and a ×10 objective lens (Brauer et al. 1992,1995). This orientation of the counting line ensured a comparable sampling because most of the non-vascular nerve fibers in the longitudinal myometrial layer run parallel to the uterine long axis. However, fine focus adjustments were required to count all the nerves located at different depths, particularly in estrogen-treated animals, although even in the hypertrophic preparations careful checking showed that nerves were visible at all depths of the preparations, i.e., there was no significant attenuation of signal with depth. The number of nerve bundles and fibers that intersected the ocular scale was counted in five areas regularly distributed along each whole-mount preparation. To standardize the degree of stretching, a factor was calculated for each whole-mount preparation by dividing the myometrium stretched width by the original unstretched width and the intercept density measurements were then corrected by this factor (Brauer et al. 1992). The intercept density of innervation is given as the mean number of nerves per millimeter of unstretched tissue. Considering that estrogen treatment provokes major changes in the size of the uterus, corrections for changes in the target size were carried out to obtain an estimation of the total nerve density. To achieve this aim, the intercept density per mm, estimated through the full depth of the preparation, was multiplied by the total width of the unstretched myometrium to give a figure proportional to the nerve density in the caudal region of the organ.

The density of innervation and diameter of blood vessels were estimated using a ×40 objective lens and an ocular scale set perpendicular to the long axis of the vessel. Three measurements per blood vessel were performed and an average of 10 vessels per animal were measured. The density of perivascular innervation is given as the mean number of fibers per millimeter of tissue and as the mean total number of nerves per vessel. Considering that blood vessels are not visible in the fresh tissue, no corrections for the degree of stretching were attempted.

Statistical Analysis

Results are expressed as the mean ± SEM. Data were compared using a one-way analysis of variance followed by the Tukey–Kramer multiple comparison test. Values of $p \leq 0.05$ were considered statistically significant.

Results

AChE Histochemistry

In prepubertal controls, cryostat tissue sections showed that AChE-positive (AChE-p) nerves penetrated into the uterus at the level of the mesometrial triangle (Figure 1A). In the caudal region of the uterine horn, AChE-p fibers were distributed in both the circular and longitudinal myometrial layers and around blood vessels located at the intramyometrial compartment (Figure 1C). Occasionally AChE-p fibers were observed in the endometrium in association with blood vessels and endometrial glands. In the cephalic region of the uterine horn, AChE-p nerves were extremely sparse and were mainly confined to the intramyometrial vascular compartment (not shown). The pattern of distribution and regional variation of AChE-p nerves observed in controls was unaffected by sympathectomy (Figure 1E), chronic estrogen treatment (Figures 1B and 1D), or combined sympathectomy and estrogen treatment (Figure 1F). However, a generalized increase in nerve diameter was observed in both intact and sympathectomized estrogen-treated animals (Figures 1B, 1D, and 1F).

In whole-mount preparations (Figures 2A–2D), uterine AChE-p nerves were organized as large individual nerve bundles (Type A) and medium-sized paravascular and free-running nerve bundles (Type B), from which thinner fibers branched toward the myometrium (Type M) and blood vessels (Type V). Measurement studies (Table 1) showed that the diameter of all these nerve types was unchanged by sympathectomy but that it was significantly increased after estrogen treatment of both intact and sympathectomized animals.

Nerve density measurements (Table 2) showed that sympathectomy did not affect the intercept density or the total density of AChE-p nerve bundles (Types A+B). In contrast, a 57% increase in the intercept density of these larger nerve bundles was observed in intact estrogen-treated animals. This increase was even more pronounced when results were corrected for changes in the width of the uterus, which showed a 1.7-fold increase after estrogen treatment (Table 2). Thickness of the estrogen-treated samples also increased substantially (data not shown). Similar increases were ob-

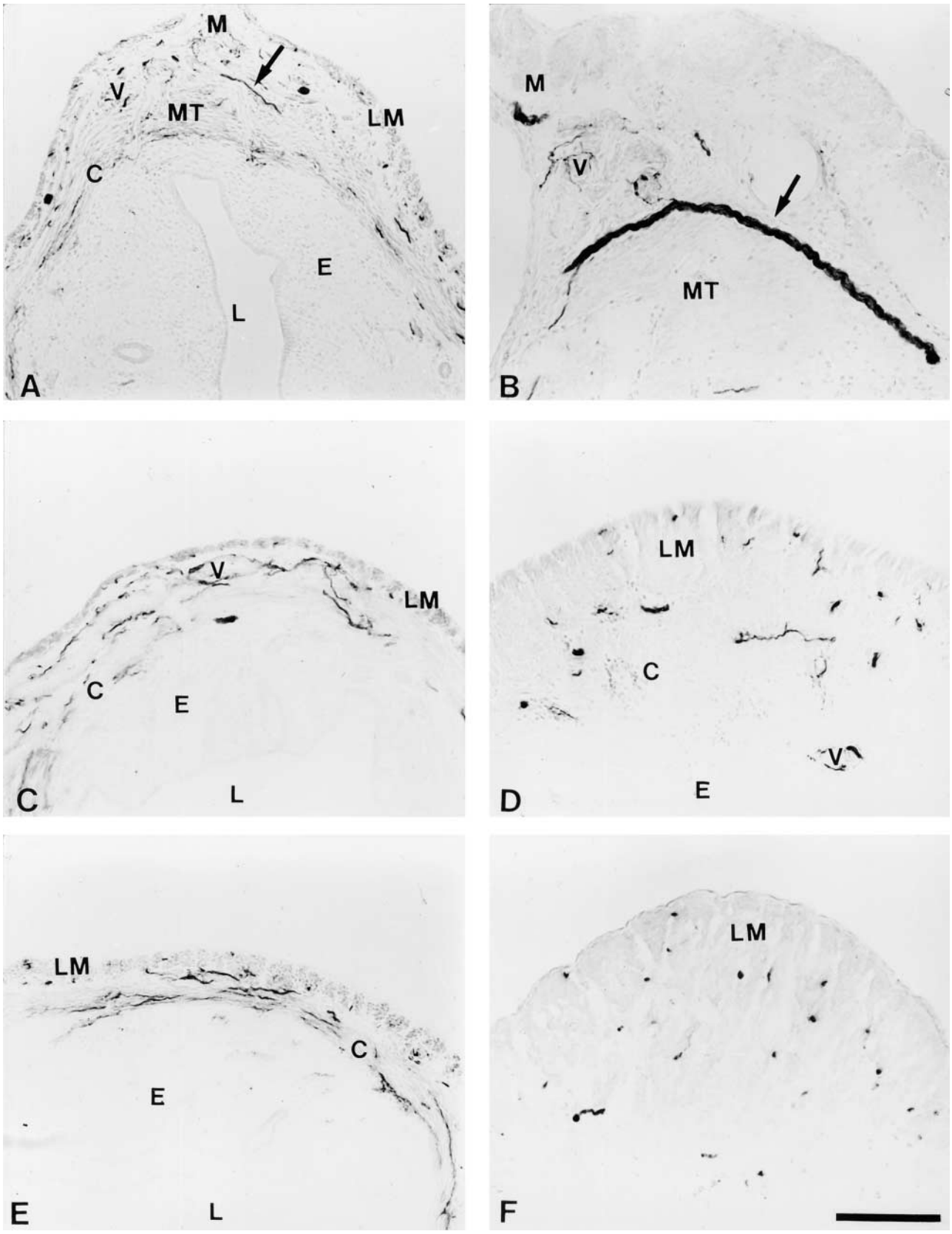
M
V
MT
LM
C
E
L
A
M
V
MT
B
V
LM
C
E
L
C
LM
C
V
E
D
LM
C
E
L
E
LM
F

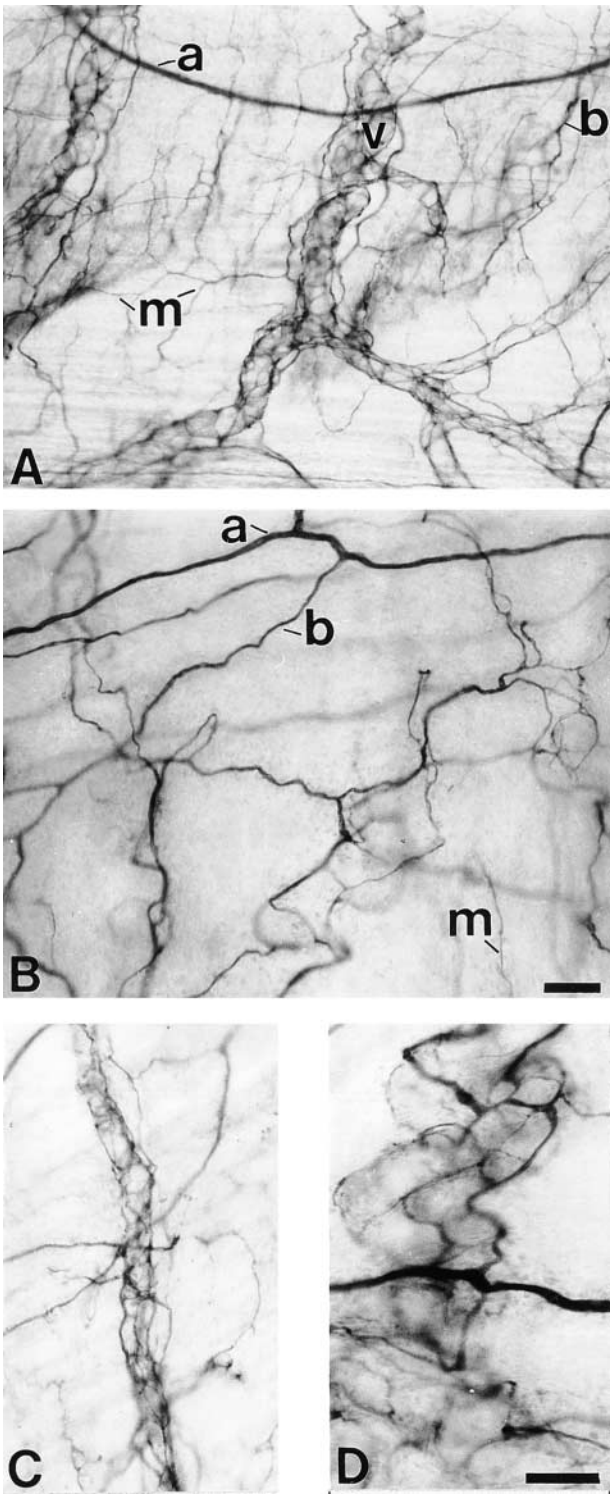

Table 1 Quantitative assessment of the effects of chemical sympathectomy with guanethidine (GTD), infantile/prepubertal chronic estrogen treatment and combined sympathectomy and estrogen treatment (GTD + EST) on the diameter (μm) of the different AChE-positive nerve types in the rat uterus[a,b]

	Control	GTD	Estrogen	GTD + EST
A	36.5 ± 1.6 (6)	34.0 ± 0.9 (3)	55.8 ± 1.6 (6)[c,d]	48.2 ± 1.8 (3)[c,d,e]
B	17.2 ± 1.5 (6)	16.7 ± 0.7 (3)	29.0 ± 1.5 (6)[c,d]	26.6 ± 0.3 (3)[c,d]
M	3.1 ± 0.5 (6)	2.3 ± 0.1 (3)	5.8 ± 0.3 (6)[c,d]	4.7 ± 0.5 (3)[d]
V	3.0 ± 0.3 (6)	1.9 ± 0.2 (3)	4.8 ± 0.4 (6)[c,d]	5.4 ± 0.2 (3)[c,d]

[a]A, thick bundles; B, medium-sized paravascular and free-running bundles; M, myometrial fibers; V, perivascular fibers.
[b]For each nerve type, data recorded from individual animals were averaged and the resulting number used to calculate mean values. An average of 100 nerves per animal were measured. Results are given as the mean ± SEM. The number of animals used for each determination is given in parentheses. Data were compared using a one-way ANOVA followed by the Tukey–Kramer multiple comparisons test. Values of $p \leq 0.05$ were considered statistically significant.
[c]Significant difference from control.
[d]Significant difference from GTD.
[e]Significant difference from estrogen.

served after chronic estrogen treatment of sympathectomized animals.

The intercept density and total density of myometrial AChE-p nerves (Type M) were unaffected by sympathectomy. After chronic estrogen treatment of intact and sympathectomized animals, a 50% reduction in the intercept density of AChE-p myometrial fibers was observed. This reduction, however, did not persist when intercept values were corrected for changes in the myometrium width, i.e., an apparent reduction in density was due to a "dilution effect" of estrogen-induced myometrial hypertrophy.

At the vascular level (Table 3), quantitative measurement showed that both the intercept density and the total number of AChE-p fibers per blood vessel were unchanged by sympathectomy. Similarly, chronic estrogen treatment of intact animals (Figures 2C and 2D) resulted in no significant changes in the total

Figure 2 Whole-mount stretch preparations illustrating the different types of acetylcholinesterase-positive nerves present in the rat uterus of control (**A**) and estrogen-treated animals (**B**). a, thick bundles (Type A); b, medium-sized bundles (Type B); m, myometrial nerve fibers (Type M); v, perivascular nerve fibers (Type V). Note the marked estrogen-induced increase in the diameter of different nerve types as well as changes in their relative density. Bar = 200 μm. (**C,D**) Estrogen-induced changes in the diameter and density of perivascular nerve fibers. Bar = 100 μm.

Figure 1 Transverse cryostat tissue sections of the caudal region of the uterine horn, showing the pattern of distribution of acetylcholinesterase-positive nerves in prepubertal rat controls (**A,C**) and after sympathectomy (**E**), prepubertal chronic estrogen treatment (**B,D**), and combined sympathectomy and chronic estrogen treatment (**F**). (**A,B**) The mesometrial triangle in control and estrogen-treated animals, respectively. (**C–F**) Pattern of distribution of intrauterine acetylcholinesterase-positive nerves in the different animal groups. Note the changes in innervation density and the increased nerve diameter in both intact and sympathectomized estrogen-treated animals (arrows). C, circular myometrial layer; E, endometrium; L, lumen; LM, longitudinal myometrial layer; M, mesometrium; MT, mesometrial triangle; V, blood vessels. Bar = 100 μm.

Table 2 Quantitative assessment of the effects of chemical sympathectomy with guanethidine (GTD), infantile/prepubertal chronic estrogen treatment, and combined sympathectomy and estrogen treatment (GTD + EST)[a]

	Control	GTD	Estrogen	GTD + EST
		Myometrium Width (mm)		
	2.52 ± 0.09 (6)	2.92 ± 0.30 (3)	4.37 ± 0.04 (6)[b,c]	4.25 ± 0.01 (3)[b,c]
		Intercept Density (nerves/mm of unstretched myometrium)		
A + B	22.7 ± 1.2 (6)	15.1 ± 5.9 (3)	35.5 ± 2.7 (6)[b,c]	30.5 ± 2.5 (3)[c]
M	139.8 ± 11.8 (6)	146.6 ± 12.2 (3)	66.6 ± 7.8 (6)[b,c]	74.5 ± 4.9 (3)[b,c]
		Total Density (total number of nerves per myometrium unstretched width)		
A + B	57 ± 3 (6)	42 ± 13 (3)	155 ± 12 (6)[b,c]	130 ± 11 (3)[b,c]
M	351 ± 33 (6)	421 ± 14 (3)	291 ± 35 (6)	317 ± 21 (3)

[a]Measurements were carried out on five areas regularly distributed along each whole-mount stretch preparation. Two to four whole-mount preparations per animal were measured. Data recorded from each animal were averaged and the resulting number used to calculate mean values. Results are given as the mean ± SEM. The number of animals used for each determination is given in parentheses. Data were compared using a one-way ANOVA followed by the Tukey–Kramer multiple comparisons test. Values of $p \leq 0.05$ were considered statistically significant. Abbreviations as in Table 1.
[b]Significant difference from control.
[c]Significant difference from GTD.

number of nerves per vessel. However, because the diameter of blood vessels was twice that measured in controls, a 46% reduction in the intercept density per millimeter of tissue was observed. After combined sympathectomy and chronic estrogen treatment, both the intercept density and the total number of AChE-p fibers per blood vessel were significantly reduced.

TH and VAChT Immunohistochemistry

In guanethidine-treated animals, no TH-immunoreactive fibers were observed in the uterus (not shown). Combined guanethidine and estrogen treatment did not alter the quality of sympathectomy.

The pattern of distribution and regional variation shown by VAChT-immunoreactive nerves (VAChT-ir) closely resembled that of AChE-positive nerves. Moreover, double-labeling experiments carried out on the same cryostat tissue sections showed that, in all animal groups, most of the nerve bundles and the perivascular and myometrial nerve fibers revealed by AChE staining were also labeled with VAChT (Figures 3A–3E). Nevertheless, varicosities appeared to be more successfully labeled with VAChT than with AchE and, very occasionally, some VAChT-ir terminal fibers were not visualized by AChE histochemistry (Figures 3D and 3F).

In both prepubertal controls and sympathectomized animals, VAChT-ir bundles and fibers were recognized in the caudal region of the uterine horn, but they were extremely rare in the cephalic region (not shown). In the caudal region (Figure 4A), VAChT-ir fibers formed a well-developed varicose plexus around blood vessels and in association with both myometrial layers. VAChT-ir fibers were particularly abundant in the circular muscle layer and in the anti-mesometrial border of the longitudinal myometrium.

After chronic estrogen treatment of intact and sympathectomized animals, several VAChT-ir bundles were recognized in the longitudinal myometrial layer and in the intramyometrial vascular space (Figures 4B and 4D). VAChT-ir varicose fibers were seen around the enlarged blood vessels and in association with both myometrial layers (Figure 4E). Examination of nerve bundles at higher magnifications showed that VAChT immunoreactivity was uneven and displayed intensely fluorescent enlargements. In controls (Figure

Table 3 Quantitative assessment of the effects of chemical sympathectmy with guanethidine (GTD), infantile/prepubertal chronic estrogen treatment, and combined sympathectomy and estrogen treatment (GTD + EST) on the blood vessel diameter (μm), perivascular intercept nerve density (fibers/mm), and total number of AChE-positive nerve fibers per vessel in the rat uterus[a]

	Control	GTD	Estrogen	GTD + EST
Vessel diameter	167 ± 4 (6)	165 ± 18 (3)	367 ± 7 (6)[b,c]	395 ± 12 (3)[b,c]
Fibers/mm	27. 4 ± 0.9 (6)	27.2 ± 2.2 (3)	14.8 ± 0.8 (6)[b,c]	7.7 ± 0.1 (3)[b,c,d]
Fibers/vessel	4.5 ± 0.2 (6)	4.3 ± 0.2 (3)	5.0 ± 0.2 (6)	2.9 ± 0.1 (3)[b,c,d]

[a]Three measurements per blood vessel were performed and an average of 10 vessels per animal were measured. Data recorded from each animal were averaged and the resulting number used to calculate mean values. The density of perivascular innervation is given as the total number of nerves per vessel and as the number of fibers per millimetre of tissue. Results are given as the mean ± SEM. The number of animals used for each determination is given in parentheses. Data were compared using a one-way ANOVA followed by the Tukey–Kramer multiple comparisons test. Values of $p \leq 0.05$ were considered statistically significant.
[b]Significant difference from control.
[c]Significant difference from GTD.
[d]Significant difference from estrogen.

4C), these structures were slightly larger than varicosities and were only occasionally recognized. In estrogen-treated animals (Figure 4F), intensely inmunofluorescent enlargements were much more prominent and abundant than in controls.

Discussion

Several studies have led to the concept that AChE staining is not a reliable marker for cholinergic nerves (Garfield 1986; Papka et al. 1999), because AChE histochemistry has also been shown to stain sympathetic (Haase et al. 1997) and primary afferent sensory nerve fibers (Papka et al. 1981). In addition, it has been demonstrated that, in several target organs, postganglionic sympathetic and parasympathetic nerve fibers run closely juxtaposed within a common Schwann cell sheath (Ehinger and Falk 1966; Ehinger et al. 1970; Elbadawi 1984; Levi 1990). Our current studies showed that neither the diameter nor the density of AChE-p nerves was affected by chronic guanethidine treatment, indicating that, in the rat uterus, AChE-p nerves are not sympathetic. The possibility that, in the caudal region of the uterine horn, some AChE-p bundles could also contain sensory nerves cannot be completely disregarded at present.

The recent generation of antibodies against the vesicular acetylcholine transporter (VAChT) has allowed specific recognition of the pattern of distribution of cholinergic nerves in different peripheral targets (Arvidson et al. 1997; Schäfer et al. 1998), including the uterus (Papka et al. 1999; Prud'homme et al. 2000). VAChT immunoreactivity appears exclusively associated with synaptic vesicles containing acetylcholine (Gilmor et al. 1996), and it has been demonstrated that VAChT is not expressed in dorsal root ganglia sensory neurons (Arvidson et al. 1997). In the present study, by double-labeling uterine cryostat tissue sections for AChE and VAChT, we observed a high degree of identity between bundles and fibers labeled by both markers. Nevertheless, it was noted that VAChT immunohistochemistry was a better marker for varicosities than AChE histochemistry. Similar differences were observed after the immunolabeling of cholinergic nerve fibers with specific antibodies against choline acetyltransferase (ChAT) and vesicular acetylcholine transporter (Papka et al. 1999). Taken together, these results indicate that, in the rat uterus, AChE staining is a good indicator of the cholinergic phenotype.

In agreement with previous studies (Adham and Schenk 1969; Moscarini et al. 1982; Papka et al. 1985; Garfield 1986; Mustafa et al. 1987; Prud'homme et al. 2000), we observed that cholinergic nerves were extremely sparse in the cephalic portion of the uterine horn but were concentrated in the caudal region, where they formed a well-developed plexus in association with blood vessels and myometrial smooth muscle. This regional pattern of distribution clearly contrasts with that shown by sympathetic (Adham and Schenk 1969; Houdeau et al. 1998; Zoubina et al. 1998) and sensory nerve fibers (Zoubina et al. 1998), which appear more concentrated in the cephalic portion of the uterine horn. This differential pattern of distribution also argues against the possibility that uterine AChE-p nerves could represent sympathetic or primary afferent sensory nerve fibers.

In marked contrast to our previous findings on sympathetic nerves (Brauer et al. 1995,1999), a well-developed plexus of cholinergic nerves was observed in the rat uterus after infantile/prepubertal chronic estrogen treatment, suggesting that developing cholinergic fibers are less affected by estrogen than sympathetic nerves. Similar results were seen in the rat during the natural estrous cycle (Zoubina et al. 1998). Moreover, our current studies showed that estrogen induced a marked increase in the diameter of cholinergic nerve bundles and fibers. It is not known, however, whether this increase in nerve size is due to an increase in the diameter of individual axons or to the recruitment of an increased number of axons per bundle. Electron microscopic studies will be required to distinguish among these and other possibilities.

Nerve density measurements showed a substantial increase in both the intercept and total density of large and medium-sized cholinergic bundles in estrogen-treated animals, suggesting that chronic exposure to estrogen during postnatal development promotes the growth of cholinergic nerves to the uterus. This increase does not appear to result from a competition with sympathetic nerves (Dahlström 1978; Aberdeen et al. 1992), because sympathectomy did not mimic the effects provoked by estrogen. Similarly, combined sympathectomy and chronic estrogen treatment did not alter the pattern of changes induced by estrogen alone.

Surprisingly, our quantitative studies demonstrated that the estrogen-induced increase in the density of large and medium-sized cholinergic nerve bundles was not reflected by a parallel increase in the intercept density of finer myometrial nerve fibers. Considering that the reduced intercept density of these nerve fibers did not persist after correction for changes in the target, it might be suggested that estrogen provoked the "dilution" of those cholinergic fibers by its hypertrophic effects on the myometrium. Dilution of the sympathetic myometrial nerve fibers that fail to keep pace with the size of the uterus was also seen in the rat during puberty (Brauer et al. 1992) and after acute (Brauer et al. 1995) and chronic exposure to estrogen of young adult rats (Chávez-Genaro et al., In press). This unusual behavior of uterine sympathetic nerves

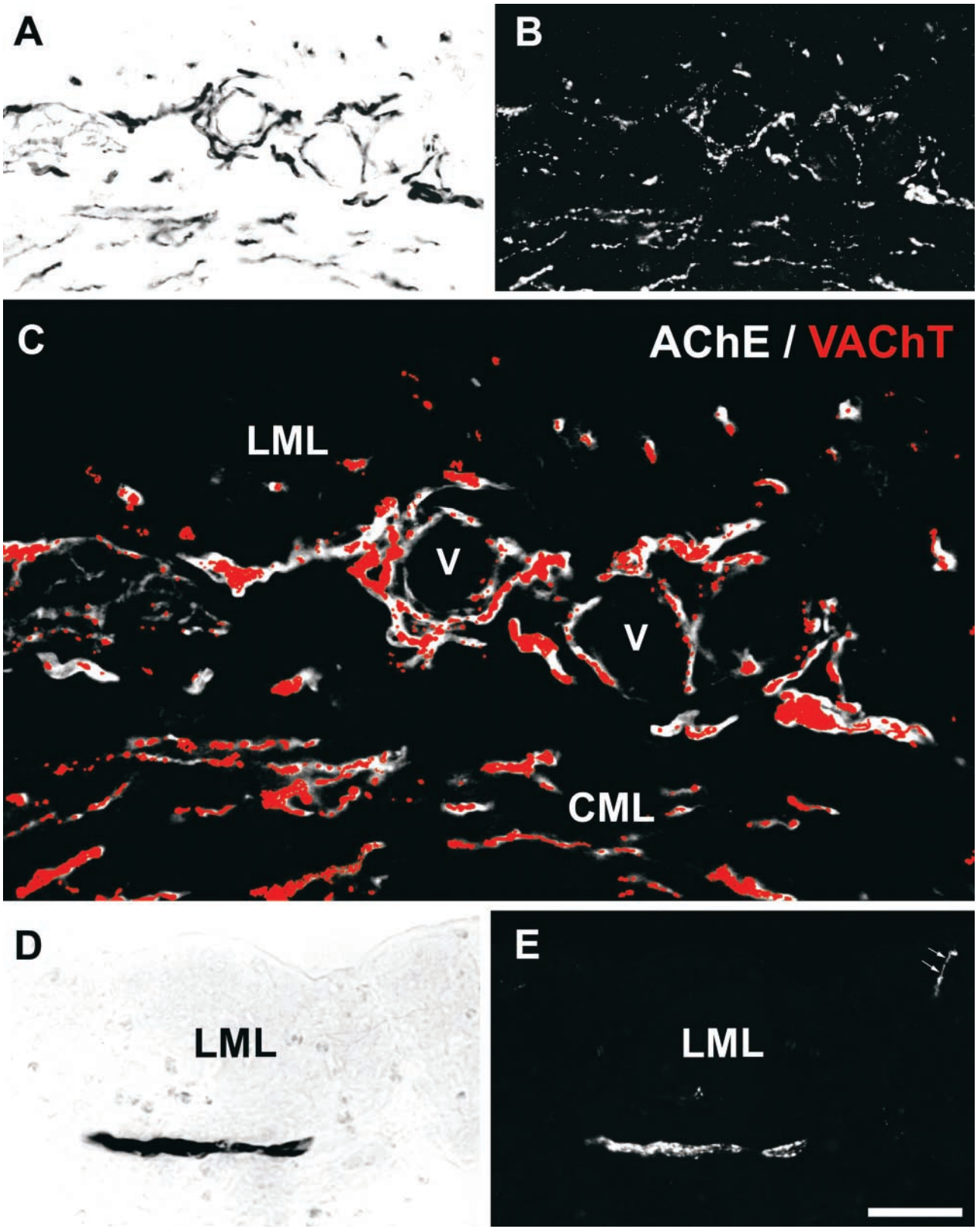
A
B
C
AChE / VAChT
LML
V
V
CML
D
LML
E
LML

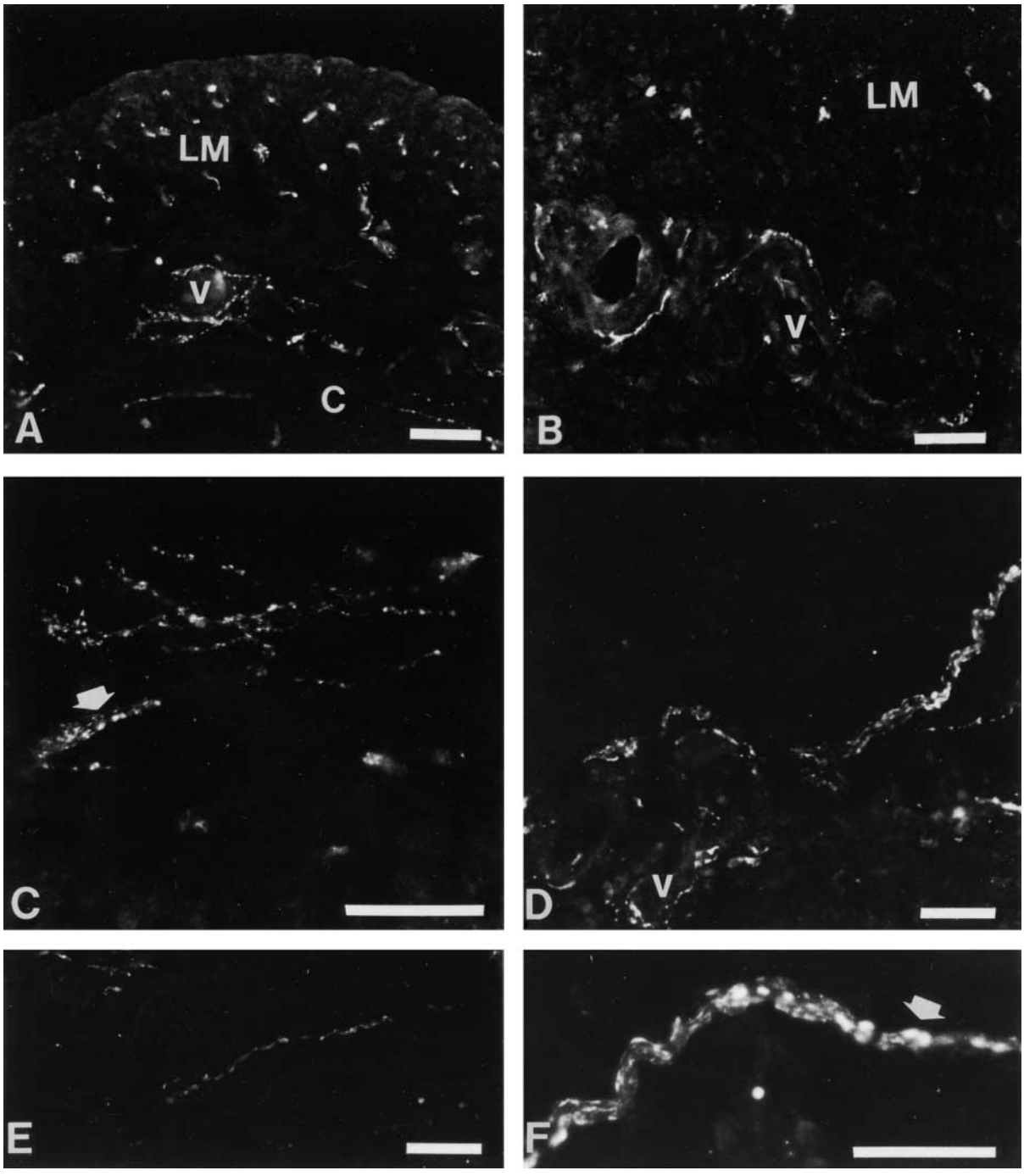

Figure 4 Transverse cryostat tissue sections showing the pattern of distribution of VAChT-immunoreactive nerves in prepubertal controls (**A,C**) and after prepubertal chronic estrogen treatment (**B,D–F**). (**E**) An "estrogen-resistant" VAChT-immunoreactive varicose fiber in the circular myometrial layer. (**C,F**) The different sizes and fluorescence intensities of VAChT immunofluorescent enlargements (arrows) is shown respectively in control and estrogen-treated animals. Bars = 100 μm.

Figure 3 Digital images of uterine cryostat tissue sections of control (**A–C**) and estrogen-treated animals (**D,E**) labeled consecutively with AChE and VAChT. Note the great similarity in the pattern of labeling given by both techniques in nerve bundles, perivascular (V), and myometrial fibers associated with the circular (CML) and longitudinal (LML) myometrial layers. (**E**) A myometrial nerve fiber labeled with VAChT is observed (double arrow). However, this fiber is not revealed by AChE histochemistry (**D**). Bars: **A,B,D,E** = 200 μm; **C** = 100 μm.

clearly contrasts with the responses of similar nerves in other hypertrophic target tissues, including muscular visceral organs, in which changes in target size induce coordinated changes in their innervating neurons (Gabella 1984; Steers et al. 1990).

Although the "dilution" explanation could account for the estrogen-induced reduction in the intercept density of myometrial nerve fibers, additional explanations can be proposed. One possible explanation is that chronic exposure to estrogen provokes the retraction or degeneration of some myometrial terminal fibers. This possibility appears to be supported by the presence of large numbers of intensely fluorescent enlargements in the VAChT-ir nerve bundles of estrogen-treated animals. These structures resemble the retraction balls observed in axons after trauma (Imajo and Roessman 1984; Emery et al. 1987; Toupalik et al. 2000), as well as the swollen varicosities observed in adrenergic (Lincoln et al. 1984), vasoactive intestinal polypeptide-immunoreactive (Belai et al. 1985), and calcitonin gene-related peptide-immunoreactive (Belai and Burnstock 1987) enteric nerve fibers of streptozotocin-induced diabetic rats. In line with this idea, it is possible that swollen or detached axons could account for the increased diameter of nerve fibers observed in estrogen-treated animals.

At the vascular level, measurement studies showed that, in intact animals, the total number of nerves per vessel was unaffected by chronic estrogen treatment. However, because the diameter of blood vessels was doubled, a 46% reduction in the density per millimeter of tissue was observed. As in the myometrium, this decrease in the intercept density of perivascular nerve fibers appears to be the result of the "dilution" of a constant number of perivascular nerve fibers over the enlarged blood vessel wall. Conversely, chronic estrogen treatment of sympathectomized animals resulted in a significant reduction in both the intercept density and the total number of AChE-p nerves per vessel, indicating that combined sympathectomy and estrogen treatment causes an actual loss of perivascular AChE-p fibers. This result suggests that, at the vascular level, degeneration of sympathetic nerves increases the effects induced by estrogen on cholinergic fibers.

The factors that prevent the coordinated growth between cholinergic terminal fibers and their target smooth muscle are not clear at present. However, it can be suggested that the growth rate of cholinergic terminal fibers is affected by estrogen-induced changes in the target tissue. This possibility is supported by our recently reported intraocular transplantation studies showing that both estrogen (Brauer et al. 2000a) and pregnancy (Brauer et al. 1998) affect the receptivity of the myometrial tissue to sympathetic nerve fibers. Although the nature of the signals produced by the target has not yet been elucidated, it is possible that sex hormones affect the pattern of growth of uterine projecting neurons via changes in the production of target-derived neurotrophic factors (Thoenen 1995; Cowen and Gavazzi 1998; Gallo and Letourneau 1998; Naves et al. 1998; Baloh et al. 2000; Brauer et al. 2000b,c; Varol et al. 2000), changes in signals provided by the extracellular matrix (de Curtis 1991; Gavazzi et al. 1995; Tessier–Lavigne and Goodman 1996), or changes in the receptivity of neurons to the signals produced by the target (Toran–Alleran 1996).

Estrogen-binding sites have been demonstrated in several neuron types of the central nervous system, where estrogen can mediate opposite effects such as neuron growth and neuroprotection (Behl and Holsboer 1999; Gibbs 2000) as well as axon atrophy (Kritzer and Kohama 1999). Alpha and beta estrogen receptor immunoreactivity and mRNA have been shown in uterine-projecting preganglionic and postganglionic parasympathetic neurons of the rat paracervical ganglia (Williams and Papka 1996; Papka et al. 1997,2001; Williams et al. 1997), which represent the main source of cholinergic nerves to the rat uterus (Papka and Traurig 1992; Papka et al. 1999; Prud'homme et al. 2000). In this context, it can be suggested that the dynamic responses induced by estrogen on developing uterine cholinergic nerves could be initiated by more than one mechanism, including a direct effect of estrogen on parasympathetic preganglionic and postganglionic neurons as well as by estrogen-induced changes in neuron–target interactions.

Our present studies indicate that chronic exposure to estrogen during the infantile/prepubertal period initiates differential responses in cholinergic and sympathetic nerves to the rat uterus. Work is in progress to elucidate the cellular and molecular mechanisms that control differential susceptibility of uterine nerves to estrogen.

Acknowledgments

Supported by The Wellcome Trust, UK (CRIG Grant 058122/Z/99/Z/JC/KO) and PEDECIBA, Universidad de la República, Uruguay.

We wish to thank Prof Keith Crutcher (Department of Neurosurgery, University of Cincinnati, Ohio) for his valuable suggestions. The assistance of Ms Aurelia Fernandez and Ms Nilda Cuña is greatly appreciated.

Literature Cited

Aberdeen J, Milner P, Lincoln J, Burnstock G (1992) Guanethidine sympathectomy of mature rats leads to increases in calcitonin gene-related peptide and vasoactive intestinal polypeptide-containing nerves. Neuroscience 47:453–461

Adham N, Schenk EA (1969) Autonomic innervation of the rat vagina, cervix and uterus and its cyclic variations. Am J Obstet Gynecol 104:508–516

Arvidsson U, Riedl M, Elde R, Meister B (1997) Vesicular acetylcho-

line transporter (VAChT) protein: a novel and unique marker for cholinergic neurons in the central and peripheral nervous system. J Comp Neurol 378:454–467

Baloh RH, Enomoto H, Johnson EM, Milbrandt J (2000) The GDNF family ligands and receptors—implications in neural development. Curr Opin Neurobiol 10:103–110

Behl C, Holsboer F (1999) The female sex hormone estrogen as a neuroprotectant. Trends Pharmacol Sci 20:441–444

Belai A, Burnstock G (1987) Selective damage of intrinsic calcitonin gene-related peptide-like immunoreactive enteric nerve fibers in streptozotocin-induced diabetic rats. Gastroenterology 92:730–734

Belai A, Lincoln J, Milner P, Crowe R, Loesch A, Burnstock G (1985) Enteric nerves in diabetic rats: increase in vasoactive intestinal polypeptide but not substance P. Gastroenterology 89:967–976

Brauer MM, Burnstock G, Thrasivoulou C, Cowen T (1998) In oculo transplants of myometrium from postpartum guinea pigs fail to support sympathetic reinnervation. J Anat 193:509–517

Brauer MM, Chávez R, Shockley K, Crutcher K, Burnstock G, Cowen T (2000c) Prepubertal chronic estrogen treatment and chemical sympathectomy with guanethidine increase NGF protein levels in the rat uterus. Autonom Neurosci Bas Clin 82:25

Brauer MM, Chávez–Genaro R, Llodrá J, Richeri A, Scorza MC (2000a) Effects of chronic estrogen treatment are not selective for uterine sympathetic nerves: a transplantation study. J Anat 196:347–355

Brauer MM, Corbacho A, Burnstock G (1995) Effects of chronic and acute estrogen treatment on the development of noradrenaline-containing nerves of the rat uterus. Int J Dev Neurosci 13:791–798

Brauer MM, Lincoln J, Blundell D, Corbacho A (1992) Postnatal development of noradrenaline-containing nerves of the rat uterus. J Autonom Nerv Syst 39:37–50

Brauer MM, Lincoln J, Milner P, Sarner S, Blundell D, Pássaro M, Corbacho A, Burnstock G (1994) Plasticity in autonomic nerves: differential effects of long-term sympathectomy on the sensory innervation of the rat uterus during maturation. Int J Dev Neurosci 12:579–586

Brauer MM, Llodrá J, Scorza MC, Chávez R, Burnstock G, Thrasivoulou C, Cowen T (1999) Differential effects of prepubertal chronic estrogen treatment on the synthesis of noradrenaline in uterine myometrial and perivascular sympathetic nerves. Int J Dev Neurosci 17:295–303

Brauer MM, Shockley KP, Chávez R, Richeri A, Cowen T, Crutcher KA (2000b) The role of NGF in pregnancy-induced degeneration and regeneration of sympathetic nerves in the guinea pig uterus. J Autonom Nerv Syst 79:19–27

Chávez-Genaro R, Crutcher K, Viettro L, Richeri A, Coirolo N, Burnstock G, Cowen T, Brauer MM (in press) Differential effects of estrogen on developing and mature uterine sympathetic nerves. Cell Tissue Res

Cowen T, Gavazzi I (1998) Plasticity in adult and ageing sympathetic neurons. Prog Neurobiol 54:249–288

Dahlström A (1978) The adrenergic innervation of the urinary bladder in the cat and man in the normal state and after parasympathetic denervation. Acta Pharmacol Toxicol 43:19–25

de Curtis I (1991) Neuronal interactions with extracellular matrix. Curr Opin Cell Biol 3:824–831

Ehinger B, Falk B (1966) Concomitant adrenergic and parasympathetic fibers in the rat iris. Acta Physiol Scand 67:201–207

Ehinger B, Falk B, Sporrong B (1970) Possible axo-axonal synapses between peripheral adrenergic and cholinergic nerve terminals. Z Zellforsch Mikrosk Anat 107:508–521

Elbadawi A (1984) Ultrastructure of vesicourethral innervation. II. Postganglionic axoaxonal synapses in intrinsic innervation of the vesicourethral lissosphincter: a new structural and functional concept of micturition. J Urol 131:781–790

Emery DG, Lucas JH, Gross GW (1987) The sequence of ultrastructural changes in cultured neurons after dendrite transection. Exp Brain Res 67:41–51

Gabella G (1984) Size of neurons and glial cells in the intramural ganglia of the hypertrophic intestine of the guinea-pig. J Neurocytol 13:73–84

Gallo G, Letourneau PC (1998) Localized sources of neurotrophins initiate axon collateral sprouting. J Neurocytol 18:5403–5414

Garfield RE (1986) Structural studies of innervation of non-pregnant rat uterus. Am J Physiol 251:C41–54

Gavazzi I, Boyle KS, Edgar D, Cowen T (1995) Reduced laminin immunoreactivity in the blood vessel wall of ageing rats correlates with reduced innervation in vivo and following transplantation. Cell Tissue Res 281:23–32

Gibbs RB (2000) Estrogen and the cholinergic hypothesis: implications for estrogen replacement therapy in postmenopausal women. In Chadwick DJ, Goode JA, eds. Novartis Foundation Symposium 230. Neuronal and Cognitive Effects of Estrogens. Chichester, John Wiley & Sons, 94–107

Gilmor ML, Nash NR, Roghani A, Edwards RH, Yi H, Hersch SM, Levey AI (1996) Expression of the putative vesicular acetylcholine transporter in the rat brain and localization in synaptic vesicles. J Neurosci 16:2179–2190

Haase EB, Buchman J, Tietz AE, Shramm LP (1997) Pregnancy-induced uterine neuronal degeneration in the rat. Cell Tissue Res 288:293–306

Hasan W, Smith PG (2000) Nerve growth factor expression in parasympathetic neurons: regulation by sympathetic innervation. Eur J Neurosci 12:1–8

Houdeau E, Rousseau A, Meusnier C, Prud'homme MJ, Rousseau JP (1998) Sympathetic innervation of the upper and lower regions of the uterus and cervix in the rat have different origins and routes. J Comp Neurol 399:403–412

Imajo T, Roessman U (1984) Diffuse axonal injury. Am J Forens Med Pathol 5:217–222

Juorio AV, Chedrese PJ, Li XM (1989) The influence of ovarian hormones on the rat oviductal and uterine concentration of noradrenaline and 5-hydroxytryptamine. Neurochem Res 14:821–827

Karnovsky MJ, Roots I (1964) A "direct" coloring thiocholine method for cholinesterases. J Histochem Cytochem 12:219–221

Kritzer MF, Kohama SG (1999) Ovarian hormones differentially influence immnunoreactivity for dopamine-beta-hydroxylase, choline acetyltransferase, and serotonin in the dorsolateral prefrontal cortex of adult rhesus monkeys. J Comp Neurol 409:438–451

Levi MN (1990) Autonomic interactions in cardiac control. Ann NY Acad Sci 601:209–221

Lincoln J, Bokor JT, Crowe R, Griffith SG, Haven AJ, Burnstock G (1984) Myenteric plexus in streptozotocin-treated rats. Gastroenterology 86:654–661

Marshall JM (1981) Effects of ovarian steroids and pregnancy on adrenergic nerves of uterus and oviduct. Am J Physiol 240: C165–174

McKercher TC, Van Orden LS, Bhatnagar RK, Burke JP (1973) Estrogen-induced biogenic amine reduction in the rat uterus. J Pharmacol Exp Ther 185:514–522

Melo RCN, Machado CRS (1993) Noradrenergic and acetylcholinesterase-positive nerve fibers of the uterus in sexually immature and cycling rats. Histochem J 25:213–218

Moscarini M, Cantagalli A, Cavalloti C, De Luca C, Amenta F (1982) Cholinergic nerves in the mouse uterus. Neural Transm 55:139–148

Mustafa F, Fatani JA, El-Eishi H, El-Badawi MG (1987) Intrinsic innervation of the uterus in guinea pig and rat. Acta Anat 129:53–58

Naves FJ, Vázquez MT, San José I, Martínez–Almagro A, Vega J (1998) Pregnancy-induced denervation of the human uterine artery correlates with local decrease of NGF and TrkA. It J Anat Embryol 103:279–290

Owman C, Stjernquist M (1988) Origin, distribution and functional aspects of aminergic and peptidergic nerves in the male and female genital tracts. In Björklund A, Hökfelt T, Owman C, eds. Handbook of Chemical Neuroanatomy. New York, Elsevier Science Publishers, 445–544

Papka RE, Cotton JP, Traurig HH (1985) Comparative distribution of neuropeptide-tyrosine-, vasoactive intestinal polypeptide-, substance P-immunoreactive and acetylcholinesterase-positive and noradrenergic nerves in the reproductive tract of the female rat. Cell Tissue Res 242:475–490

Papka RE, Furness JB, Dell NG, Costa M (1981) Depletion by capsaicin of substance-P-immunoreactive and acetylcholinesterase activity from nerve fibers in the guinea pig heart. Neurosci Lett 27:47–53

Papka RE, Srinivasan B, Miller KE, Hasashi S (1997) Localization of estrogen receptor protein and estrogen receptor messenger RNA in peripheral autonomic and sensory neurons. Neuroscience 79:1153–1163

Papka RE, Storey–Workley M, Shughrue PJ, Merchenthaler I, Collins JJ, Usip S, Saunders PT, Shupnik M (2001) Estrogen receptor-alpha and beta-immunoreactivity and mRNA in neurons of sensory and autonomic ganglia and spinal cord. Cell Tissue Res 304:193–214

Papka RE, Traurig HH (1992) Autonomic and visceral sensory innervation of the female reproductive system: special reference to neurochemical markers in nerves and ganglionic connections. In Maggi CA, ed. Nervous Control of the Urogenital System. Basel, Harwood Academic Publishers, 423–436

Papka RE, Traurig HH, Scheman M, Collins J, Copelin T, Wison K (1999) Cholinergic neurons of pelvic autonomic ganglia and uterus of the female rat: distribution of axons and presence of muscarinic receptors. Cell Tissue Res 269:293–305

Prud'homme MJ, Houdeau E, Rossano B (2000) Regional differences in the distribution of cholinergic nerve fibers along the uterus in the rat. Functional implications. Autonom Neursci Bas Clin 82:75

Schäfer MKH, Eiden LE, Weihe E (1998) Cholinergic neurons and terminal fields revealed by immunohistochemistry for the vesicular acetylcholine transporter. II. The peripheral nervous system. Neuroscience 84:361–376

Sharp CE, Smith PG (1992) Developmental regulation of parasympathetic nerve density by sympathetic innervation in the tarsal smooth muscle of the rat. Neuroscience 49:229–236

Smith PG, Marzban F (1998) Parasympathetic varicosity proliferation and synaptogenesis in rat eyelid smooth muscle after sympathectomy. Brain Res 786:171–180

Steers WD, Ciambotti J, Erdman S, de Groat WC (1990) Morphological plasticity in efferent pathways to the urinary bladder of the rat following urethral obstruction. J Neurosci 10:1943–1951

Stjernquist M, Alm P, Ekman R, Owman C, Sjöberg NO, Sundler F (1985) Levels of neural vasoactive intestinal polypeptide in the rat uterus are markedly changed in association with pregnancy as shown by immunohistochemistry. Biol Reprod 33:157–163

Tessier–Lavigne M, Goodman CS (1996) The molecular biology of axon guidance. Science 274:1123–1133

Thoenen H (1995) Neurotrophins and neuronal plasticity. Science 270:593–598

Toran–Alleran CD (1996) The estrogen/neurotrophin connection during neural development: is co-localization of estrogen receptors whith neurotrophins and their receptors biologically relevant? Dev Neurosci 18:36–48

Toupalik P, Klir P, Bouska I, Chadova L (2000) Immunohistochemical methods in differential diagnosis of primary traumatic and subsequent secondary cerebral changes. Soud Lek 45:18–21

Traurig HH, Papka RE (1992) Autonomic and visceral sensory innervation of the female reproductive system: special reference to the functional roles of nerves in reproductive functions. In Maggi CA, ed. Nervous Control of the Urogenital System. Basel, Harwood Academic Publishers, 103–141

Varol FG, Duchemin AM, Neff HN, Hadjiconstantinou M (2000) Nerve growth factor (NGF) and NGF mRNA change in rat uterus during pregnancy. Neurosci Lett 294:58–62

Williams SJ, Chung K, Om AS, Papka RE (1997) Cytosolic estrogen receptor concentrations in the lumbosacral spinal cord fluctuate during the estrous cycle. Life Sci 61:2551–2559

Williams SJ, Papka RE (1996) Estrogen receptor-immunoreactive neurons are present in the female rat lumbosacral spinal cord. J Neurosci Res 46:492–501

Zoubina EV, Fan Q, Smith PG (1998) Variation in uterine innervation during the estrous cycle. J Comp Neurol 397:561–571

Zoubina EV, Mize AL, Alper RH, Smith PG (2001) Acute and chronic estrogen supplementation decreases uterine sympathetic innervation in ovariectomised adult virgin rats. Histol Histopathol 16:989–996